

Article

# Phenethyl Isothiocyanate Inhibits In Vivo Growth of Xenograft Tumors of Human Glioblastoma Cells

Yu-Cheng Chou<sup>1,2,3</sup>, Meng-Ya Chang<sup>4</sup>, Hsu-Tung Lee<sup>1,5</sup>, Chiung-Chyi Shen<sup>1,6</sup>,  
Tomor Harnod<sup>7,8</sup>, Yea-Jiuan Liang<sup>1</sup>, Rick Sai-Chuen Wu<sup>9,10</sup>, Kuang-Chi Lai<sup>11</sup>,  
Fei-Ting Hsu<sup>12,\*,†</sup> and Jing-Gung Chung<sup>12,13,\*,†</sup>

<sup>1</sup> Department of Neurosurgery, Neurological Institute, Taichung Veterans General Hospital, Taichung 40754, Taiwan; chouycns@yahoo.com.tw (Y.-C.C.); leesd2001@gmail.com (H.-T.L.); shengeorge@yahoo.com (C.-C.S.); shelby63liang@gmail.com (Y.-J.L.)

<sup>2</sup> Department of Neurological Surgery, Tri-Service General Hospital, National Defense Medical Center, Taipei 114, Taiwan

<sup>3</sup> Rong Hsing Research Center for Translational Medicine, National Chung Hsing University, Taichung 402, Taiwan

<sup>4</sup> Institute of Medical Sciences, Tzu Chi University, Hualien 970, Taiwan; mchang@mail.tcu.edu.tw

<sup>5</sup> Graduate Institute of Medical Sciences, National Defense Medical Center, Taipei 11490, Taiwan

<sup>6</sup> Department of Physical Therapy, Hung Kuang University, Taichung 43302, Taiwan

<sup>7</sup> Department of Neurosurgery, Hualien Tzu Chi General Hospital, Buddhist Tzu Chi Medical Foundation, Hualien 970, Taiwan; tomorha@yahoo.com.tw

<sup>8</sup> College of Medicine, Tzu Chi University 970, Hualien, Taiwan

<sup>9</sup> Department of Anesthesiology, China Medical University Hospital, Taichung 404, Taiwan; rickwu@mail.cmuh.org.tw

<sup>10</sup> Department of Anesthesiology, China Medical University, Taichung 40402, Taiwan

<sup>11</sup> Department of Medical Laboratory Science and Biotechnology, College of Medicine and Life Science, Chung Hwa University of Medical Technology, Tainan 71703, Taiwan; kuangchi\_lai@hotmail.com

<sup>12</sup> Departments of Biological Science and Technology, China Medical University, Taichung 40402, Taiwan

<sup>13</sup> Department of Biotechnology, Asia University, Taichung 413, Taiwan

\* Correspondence: sakiro920@mail.cmu.edu.tw (F.-T.H.); jgchung@mail.cmu.edu.tw (J.-G.C.); Tel.: +886-4-2205-3366 (ext. 8000) (J.-G.C.); Fax: +886-4-2205-3764 (J.-G.C.)

† These authors contributed equally to this work.

Received: 24 July 2018; Accepted: 4 September 2018; Published: 10 September 2018



**Abstract:** Phenethyl isothiocyanate (PEITC) from cruciferous vegetables can inhibit the growth of various human cancer cells. In previous studies, we determined that PEITC inhibited the in vitro growth of human glioblastoma GBM 8401 cells by inducing apoptosis, inhibiting migration and invasion, and altering gene expression. Nevertheless, there are no further in vivo reports disclosing whether PEITC can suppress the growth of glioblastoma. Therefore, in this study we investigate the anti-tumor effects of PEITC in a xenograft model of glioblastoma in nude mice. Thirty nude mice were inoculated subcutaneously with GBM 8401 cells. Mice with one palpable tumor were divided randomly into three groups: control, PEITC-10, and PEITC-20 groups treated with 0.1% dimethyl sulfoxide (DMSO), and 10 and 20  $\mu$ mole PEITC/100  $\mu$ L PBS daily by oral gavage, respectively. PEITC significantly decreased tumor weights and volumes of GBM 8401 cells in mice, but did not affect the total body weights of mice. PEITC diminished the levels of anti-apoptotic proteins MCL-1 (myeloid cell leukemia 1) and XIAP (X-linked inhibitor of apoptosis protein) in GBM 8401 cells. PEITC enhanced the levels of caspase-3 and Bax in GBM 8401 cells. The growth of glioblastoma can be suppressed by the biological properties of PEITC in vivo. These effects might support further investigations into the potential use of PEITC as an anticancer drug for glioblastoma.

**Keywords:** phenethyl isothiocyanate; apoptosis; xenograft; caspase; glioblastoma

## 1. Introduction

Aside from surgery, chemotherapy with the alkylating agent temozolomide and radiotherapy are first-line therapies for glioblastoma, but their survival benefits are short-lived and the tumors may develop resistance to therapies [1]. This most common and aggressive primary brain malignancy cannot be well-controlled by the current multimodality treatments. Phenethyl isothiocyanate (PEITC), a component in cruciferous vegetables, has chemopreventive activity for various tumors [2], and has also been applied in small human clinical trials against different diseases from cancer to autism [3]. The antitumor effect of PEITC has been discussed in numerous studies. In carcinogenesis, the epigenetic modification of DNA and histone proteins by methylation and deacetylation is one of the key factors [4]. A study by Cang et al. confirmed that PEITC can be used as a histone deacetylase (HDAC) inhibitor in various tumors (e.g., prostate cancer, breast cancer, leukemia, and myeloma cells) [5]. Hypoacetylated, hypomethylated, and dephosphorylated forms of the histone H2B in DU-145 prostate cancer cells can be reversed by HDAC inhibitors [6]. The inhibition of HDACs and DNA methyltransferases has been used as novel cancer therapy strategies for epigenetic modification in acute myeloid leukemia [7]. Although PEITC has shown promising anti-cancer effects in clinical trials on leukemia [8], the toxicity effects of PEITC were mainly evaluated on liquid tumors and not solid tumors. Our previous studies revealed the *in vitro* effects of PEITC on human glioblastoma GBM 8401 cells: (1) inducing apoptosis through the extrinsic (death receptor) pathway, dysfunction of mitochondria, reactive oxygen species (ROS)-induced endoplasmic reticulum (ER) stress, and the intrinsic (mitochondrial) pathway in GBM 8401 cells [9]; (2) suppressing migration and invasion through the inhibition of uPA, Rho A, and Ras with inhibition of MMP-2, -7, and -9 gene expression [10]; (3) altering the gene expressions and the levels of protein associated with cell cycle regulation [11]. However, the function of PEITC in various cancer-promoting mechanisms, including cell proliferation, progression, and metastasis, in living subjects with glioblastoma remains ambiguous.

There are no reports in the available literature disclosing that PEITC inhibits the growth of glioblastoma *in vivo*. In the present study, we first investigated the anti-tumor effects of PEITC in a xenograft model of glioblastoma in nude mice.

## 2. Results

### 2.1. PEITC Did Not Affect the Body Weights in Xenograft GBM 8401/*luc2* Cells-Bearing Animal Models

The body weights of each group were measured every 3 days, and the results are shown in Figure 1. Notably, no significant difference of body weight change was seen among the control, PEITC-10 (10  $\mu$ mole PEITC/100  $\mu$ L PBS), and PEITC-20 (20  $\mu$ mole PEITC/100  $\mu$ L PBS) groups (Figure 1), which indicated no signs of acute or delayed toxicity of PEITC.

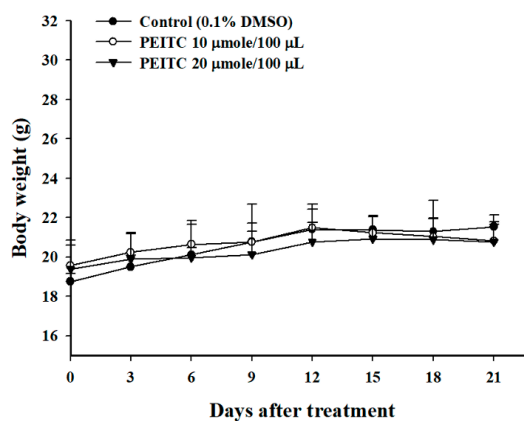


**Figure 1.** The effects on body weight in xenograft GBM 8401/*luc2* cells-bearing mouse models. The body weights of mice treated with phenethyl isothiocyanate (PEITC) remained similar to those of control mice throughout the study period.

### 2.2. PEITC Inhibited Xenograft Tumor Growth of GBM 8401/luc2 Cells

Ectopic tumor-bearing nude mice were treated with vehicle and PEITC at different concentrations for 21 days, and they were anesthetized with 1–3% isoflurane every 1 week during scanning. The efficacy of the treatment was evaluated by bioluminescent imaging (BLI) (Figure 2A). Photons emitted from the tumors of the PEITC-10 group were significantly lower than those of the control group, and those emitted from the tumors of PEITC-20 group were significantly lower than those of the PEITC-10 group (Figure 2B). These results suggested that both doses of PEITC reduced the total photon flux significantly in comparison with control group, and the higher dose of PEITC led to a lower total photon flux than did the lower dose of PEITC.

The tumor volume of each mouse was measured every 3 days during treatments for 21 days, and six representative tumors from three groups were extracted as shown in Figure 2C,D. These indicated that both doses of PEITC significantly decreased the tumor volumes in comparison with the control group, and the higher dose of PEITC resulted in lower tumor volumes than did the lower dose of PEITC. Both doses of PEITC also significantly reduced the tumor weights in comparison with the control group, and the higher dose of PEITC led to lower the tumor weights than did the lower dose of PEITC (Figure 2E).

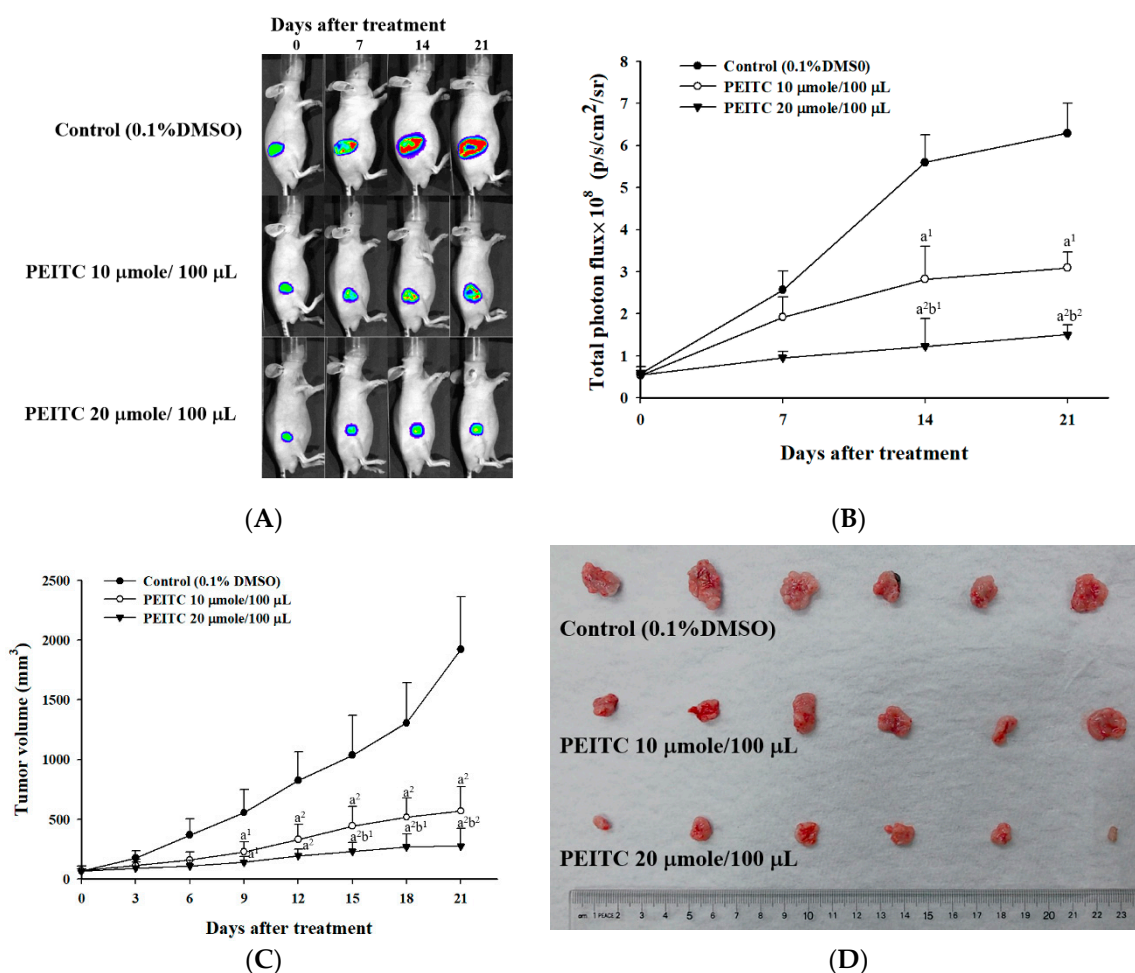
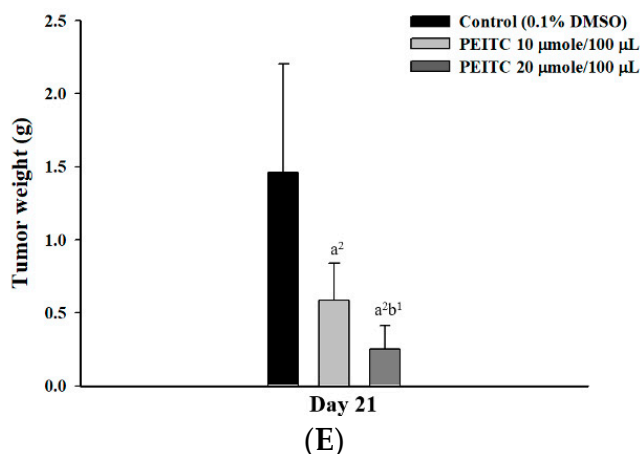


Figure 2. Cont.



**Figure 2.** Therapeutic efficacy evaluation of PEITC in xenograft GBM 8401/*luc2* cells-bearing mice. (A) The tumor growth of each mouse was monitored by bioluminescent imaging (BLI) every one week. The tumor growth was significantly suppressed by PEITC at both doses (PEITC-10, PEITC-20) compared to the control group. (B) The regions-of-interest (ROIs) of tumors in (A) were quantified. The PEITC-20 group revealed the most obvious tumor inhibition. a<sup>1</sup>:  $p < 0.05$ , a<sup>2</sup>:  $p < 0.01$  compared to that of the control; b<sup>1</sup>:  $p < 0.05$ , b<sup>2</sup>:  $p < 0.01$  compared to that of PEITC-10 group. (C) The tumor volumes of each mouse were assayed by caliper measurement every 3 days. The tumor volumes were significantly reduced by PEITC at both doses (PEITC-10, PEITC-20 groups) compared to the control group. a<sup>1</sup>:  $p < 0.05$ , a<sup>2</sup>:  $p < 0.01$  compared to that of the control; b<sup>1</sup>:  $p < 0.05$ , b<sup>2</sup>:  $p < 0.01$  compared to that of PEITC-10 group. (D) Six representative tumor pictures from each group are displayed after the mice were sacrificed. (E) The tumor weights of each mouse were assayed after they were sacrificed on day 21. The tumor weights were significantly decreased by PEITC at both doses (PEITC-10, PEITC-20 groups) compared to the control group. a<sup>2</sup>:  $p < 0.01$  compared to that of the control; b<sup>1</sup>:  $p < 0.05$  compared to that of PEITC-10 group.

### 2.3. PEITC Altered Apoptosis Associated Proteins Signaling in Xenograft Tumor of GBM 8401/*luc2* Cells

All samples were observed under microscopy at  $\times 100$  magnification after immunohistochemical (IHC) staining. Five regions of each slide were randomly selected for photographing (Figure 3A). Results indicated that the samples at both doses of PEITC were weakly stained with anti-MCL-1 (myeloid cell leukemia 1) and -XIAP (XIAP (X-linked inhibitor of apoptosis protein)) compared to the control group (Figure 3A). The higher dose of PEITC (20  $\mu\text{mole}/100 \mu\text{L}$  PBS/day) led to lower staining with anti-MCL-1 and -XIAP than the low dose of PEITC (10  $\mu\text{mole}/100 \mu\text{L}$  PBS/day). The samples at both doses of PEITC were strongly stained with anti-caspase-3 and -Bax compared to the control group (Figure 3B). The higher dose of PEITC resulted in higher staining with anti-caspase-3 and -Bax than did the low dose of PEITC. The quantification of MCL-1, XIAP, caspase-3, and Bax proteins expression was performed by Image J software (Madison, WI, USA), respectively (Figure 3C,D). Thus, PEITC changed the expressions of apoptosis-associated proteins in the signal pathway of GBM 8401/*luc2* cells in vivo.

### 2.4. Effects of PEITC on the Hepatic Histopathological Change in GBM 8401/*luc2* Cell Xenograft Animal Model

Liver was collected from every mouse of every group after treatment, embedded in paraffin, sectioned into 5  $\mu\text{m}$ -thick slices, deparaffinized, and stained with hematoxylin and eosin (H&E). Liver specimens from PEITC-treated and control groups revealed similar hepatocyte arrangement in hepatocytes and lobular architectures (Figure 4).

There were no significant differences in mice liver between PEITC-treated and control groups, so there was no obvious hepatic cytotoxicity after PEITC treatment GBM 8401/*luc2* cells in vivo.

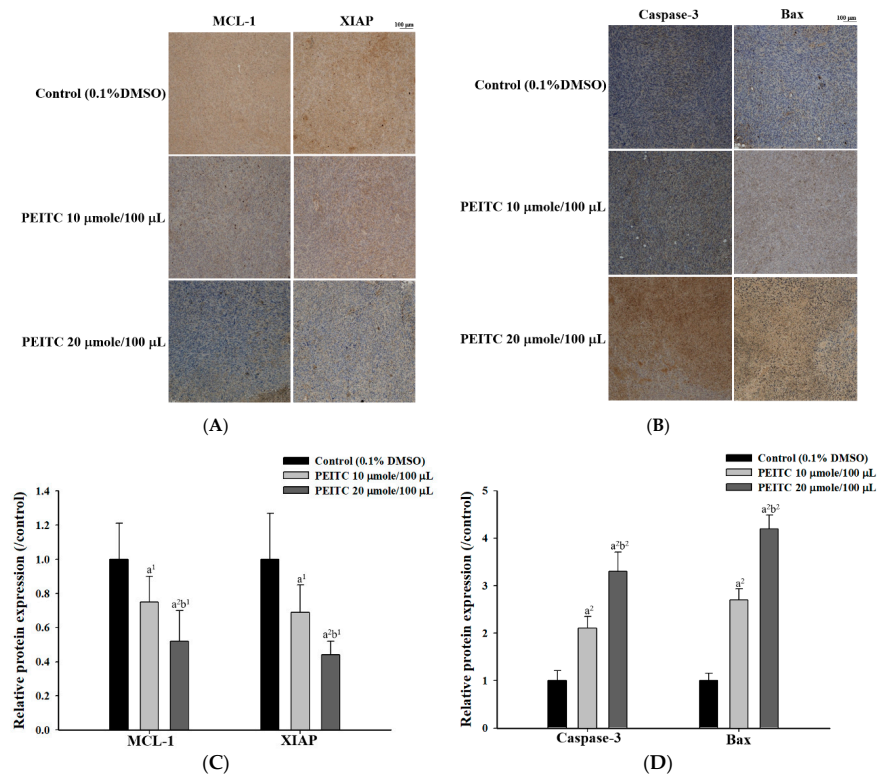


**Figure 3.** The effects of PEITC on the expressions of apoptosis-associated proteins in xenograft GBM 8401/*luc2* cells-bearing mice. Tumors were isolated from xenograft GBM 8401/*luc2* cells-bearing mice after treatment. All samples were analyzed under microscopy at  $\times 100$  magnification and photographed. **(A)** MCL-1 (myeloid cell leukemia 1) and XIAP (X-linked inhibitor of apoptosis protein); **(B)** Caspase-3 and Bax. **(C)** Quantification results of MCL-1 and XIAP. **(D)** Quantification results of Caspase-3 and Bax.  $a^1$ :  $p < 0.05$ ,  $a^2$ :  $p < 0.01$  compared to that of the control;  $b^1$ :  $p < 0.05$ ,  $b^2$ :  $p < 0.01$  compared to that of PEITC-10 group.

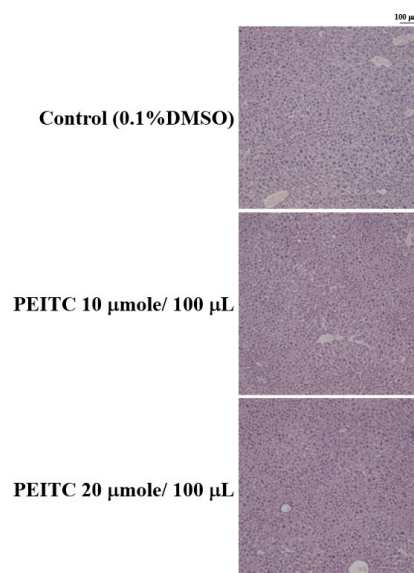


**Figure 4.** The effects of PEITC on liver histopathology in GBM 8401/*luc2* cells xenograft animal model. Liver tissue from every mouse of every group after treatment was collected and stained with hematoxylin and eosin (H&E). Liver specimens from PEITC-treated and control groups revealed similar structures of hepatocytes and lobular architectures.

### 3. Discussion

PEITC reduced tumor weights, but did not affect total body weights in subcutaneous xenograft tumors of human malignant melanoma A375.S2 cells-bearing mice *in vivo* [12]. In the present study, PEITC also did not affect total body weights in xenograft GBM 8401/*luc2* cells-bearing mice (Figure 1). However, PEITC did reduce the tumor growth in xenograft GBM 8401/*luc2* cells-bearing mice (Figure 2). PEITC had *in vivo* effects on different mouse cancer models [13]. The growth arrest of prostate cancer cells can be induced by miR-130b~301b cluster overexpression through the epigenetic regulation of proliferation-blocking genes and the activation of cellular senescence [14]. It was chemopreventive to normalize microRNAs of which downregulation was epigenetically induced by environmental cigarette smoke in a Sprague-Dawley rat lung cancer model [15]. In the azoxymethane (AOM)-initiated and dextran sodium sulfate (DSS)-promoted-C57BL/6 mice colon cancer model, PEITC inhibited colon tumor multiplicity and intestinal polyp development, and reduced intestinal tumor size associated with apoptosis (enhanced cleaved caspase-3 and -7) and cell cycle arrest (elevated p21) [16]. Therefore, PEITC had *in vivo* effects on different cancer models including glioblastoma, melanoma, lung, and colon cancers.

In our previous study, PEITC could induce apoptosis of human brain glioblastoma GBM 8401 cells through the extrinsic and intrinsic signaling pathways *in vitro* [9]. PEITC decreased anti-apoptotic protein MCL-1, and inhibited XIAP *in vitro*. In the present study, both doses of PEITC reduced the levels of MCL-1 and XIAP in GBM 8401 cells *in vivo* (Figure 3A). The anti-apoptotic MCL-1 is a key regulator in cancer cell survival, and can be a therapeutic target [17,18]. In the highly aggressive U87-EGFRvIII model and a patient-derived xenograft system, sorafenib suppressed MCL-1 expression by combining with validated compounds of histone deacetylase (HDAC) inhibitor and Bromodomain protein (BRD) inhibitor, and facilitated apoptosis from the combination treatment *in vivo* [19]. Additionally, PEITC is also known to act as a HDAC inhibitor in prostate cancer, leukemia, and myeloma cells [5–7]. HDAC inhibitors have been approved to treat T-cell lymphomas, and in many clinical trials for other hematologic and solid cancers (over 500 studies in [clinicaltrials.gov](http://clinicaltrials.gov)) [20]. Multiple histone modifications changing global gene expression might be involved in certain cancers, so the effects of combination therapy targeting two or more associated epigenetic changes could be synergistic [20]. In murine model systems of patient-derived orthotopic xenografts of human glioblastoma, breast cancer, and melanoma *in vivo*, and human glioblastoma U87MG, LN229, U251, T98G cells *in vitro*, the tumor growth can be degraded by the inhibition of histone deacetylase, mitochondrial matrix chaperones, and anti-apoptotic B-cell lymphoma 2 (Bcl-2) proteins including Bcl-2, Bcl-xL, and MCL-1 [19,21,22]. PEITC also inhibited the tumor growth by inhibiting MCL-1 in our GBM 8401 ectopic xenografts *in vivo* (Figure 3A).

Inhibitor of apoptosis proteins (IAPs) are anti-apoptotic proteins including cIAP1 (cellular inhibitor of apoptosis protein-1), cIAP2 (cellular inhibitor of apoptosis protein-2), XIAP and ML-IAP (melanoma inhibitor of apoptosis protein), and facilitate treatment resistance by inhibiting caspase activation [23]. XIAP degradation was induced and the NF- $\kappa$ B pathway was inhibited by 3-((decahydronaphthalen-6-yl)methyl)-2,5-dihydroxycyclohexa-2,5-diene-1,4-dione (RF-Id), which led to the cleavage of caspases 8, 9, 3, and 7, and blocked c-IAP2/XIAP interaction in human glioblastoma U87MG and LN229 cells *in vitro* [24]. The caspase-dependent apoptosis in glioblastoma cells can be induced by RF-Id by inhibiting IAP family proteins and the NF- $\kappa$ B pathway. GDC-0152, a SMAC (second mitochondria-derived activator of caspases) mimetic antagonizing these IAPs, affected human glioblastoma U87MG orthotopic xenografts in a dose-dependent manner. It delayed tumor formation, slowed down tumor growth *in vivo*, and thereafter improved the survival of GBM-bearing mice [25]. PEITC also inhibited tumor growth by inhibiting XIAP in our GBM 8401 ectopic xenografts *in vivo* (Figure 3A).

PEITC increased the levels of caspase-3, -9, -8, -2 and -4 of GBM 8401 cells *in vitro* [9], and both doses of PEITC elevated the levels of caspase-3 and Bax of GBM 8401 cells *in vivo* in the present study (Figure 3B). The higher dose of PEITC resulted in higher levels of caspase-3 and Bax in GBM 8401 cells

in vivo. The induction of apoptosis involves the Fas receptor and the activation of initiator caspases (caspase-8 and -9) as well as an executioner caspase (caspase-3) [22,26,27]. The expressions of cell cycle regulator Cdk1 (cyclin-dependent kinase 1) and anti-apoptotic protein Bcl-2 were decreased, and the expression of Bax and cleavage of PARP (poly ADP ribose polymerase) proteins were increased by the synergistic effects of the epigenetic agent PEITC and the chemotherapeutic agent paclitaxel (taxol) in breast cancer cells [5]. The levels of pro-apoptotic Bax and cleaved caspase-3 were enhanced, and Bcl-2 expression was downregulated from leucine-rich  $\alpha$ 2 glycoprotein 1 (LRG1)-silencing, which inhibited the growth of xenograft tumors and induced apoptosis of U251 glioblastoma cells in vitro and in vivo [28]. The increased levels of caspase-3 or Bax can be discovered in the apoptosis of different glioblastoma cell lines in vitro and in vivo. PEITC inhibited tumor growth by enhancing caspase-3 and Bax in our GBM 8401 ectopic xenografts in vivo.

In the present study, there were no significant differences in mouse liver between PEITC-treated and control groups, so there was no obvious hepatic cytotoxicity after PEITC treatment of GBM 8401/*luc2* cells in vivo (Figure 4). In the Sprague-Dawley rat model, the activity and protein levels of hepatic glutathione S-transferases (GSTs) were increased in a dose-dependent manner after treatment with PEITC [29]. On the contrary, PEITC may have a protective function against hepatotoxicity of acetaminophen through its induction effect on GST. It might be safe to use PEITC in animal model of glioblastoma and the development of potential anticancer agents.

Taken together, PEITC can diminish the ectopic xenograft tumor growth of GBM 8401 cells in tumor weights and volumes, which may be through the induction of apoptosis by the decrease of anti-apoptotic proteins MCL-1 and XIAP, and the increase of pro-apoptotic proteins caspase-3 and Bax. The in vivo effects of PEITC on the growth of GBM 8401 cells might contribute to new insights into anti-tumor treatment for glioblastoma.

## 4. Materials and Methods

### 4.1. Chemicals and Reagents

PEITC, Tris-HCl, trypan blue, and dimethyl sulfoxide (DMSO) were purchased from Sigma Chemical Co. (St. Louis, MO, USA). RPMI-1640, fetal bovine serum (FBS), L-glutamine, penicillin-streptomycin, and trypsin-EDTA were obtained from Gibco BRL/Invitrogen (Carlsbad, CA, USA). The primary antibodies and secondary antibody, anti-MCL-1 (myeloid cell leukemia 1), anti-XIAP (X-linked inhibitor of apoptosis protein), anti-caspase-3, and anti-Bax, and anti-goat IgG were obtained from Cell Signaling Technology (Irvine, CA, USA) and Amersham Pharmacia Biotech, Inc. (Piscataway, NJ, USA), respectively. PEITC was dissolved in DMSO.

### 4.2. Cell Culture

Human brain glioblastoma multiforme (GBM 8401) cell line was purchased from the Food Industry Research and Development Institute (Hsinchu, Taiwan) and cultured according to the provider's instructions. Cells were cultured in RPMI 1640 medium supplemented with 10% fetal bovine serum (FBS), 2 mM L-glutamine, 100 Units/mL penicillin, and 100  $\mu$ g/mL streptomycin and grown at 37 °C under a humidified 5% CO<sub>2</sub> and 95% air at one atmosphere. The medium was changed every 2 days [30].

### 4.3. Transfection and Stable Clone Selection

We transfected GBM 8401 cells with the plasmid of pGL4.50 luciferase reporter (pGL4.50 [*luc2*/CMV]) vector using JetPEI™ transfection reagent (Polyplus transfection, New York, NY, USA) [31]. The plasmid of pGL4.50 luciferase reporter (pGL4.50[*luc2*/CMV]) was obtained from Promega (Madison, WI, USA). Stable clone was selected by two-week treatment of 200  $\mu$ g/mL hygromycin and validated by a Xenogen IVIS imaging system (Xenogen, Alameda, CA, USA). Luciferase expressing stable clone was finally named as GBM8401/*luc2*.

#### 4.4. Animals and Treatments

Six-week-old male athymic CAnN.Cg-Foxn1<sup>nu</sup>/CrI NarI nude mice were bought from the National Laboratory Animal Center, Taipei, Taiwan. All studies followed the National Institutes of Health Guidelines for Animal Research, and were approved by the Institutional Animal Care and Use Committee of Taipei Medical University (number: LAC-2017-0248). GBM8401/*luc2* cells ( $1 \times 10^7$ ) in 150  $\mu$ L mixture containing serum-free RPMI and Matrigel (2:1) were subcutaneously inoculated into the right hind legs of the 30 mice [32]. We measured the tumor volume of each animal with a digital caliper and calculated with the equation: tumor volume =  $0.523 \times \text{length} \times \text{width}^2$  [33]. After the tumor volume reached 100–120 mm<sup>3</sup>, mice were randomized into three different treatment groups (n = 10 for each group), including vehicle, PEITC-10 group, and PEITC-20. The vehicle group was treated with 110  $\mu$ L phosphate-buffered saline (PBS) plus 10  $\mu$ L DMSO by gavage daily for 21 days. PEITC-10 and PEITC-20 groups were treated with PEITC 10  $\mu$ mole/100  $\mu$ L PBS/day and PEITC 20  $\mu$ mole/100  $\mu$ L PBS/day for 21 days, respectively. We monitored the tumor growth with bioluminescent imaging (BLI) and caliper. The body weights and tumor volumes of mice were measured 3 times per week after treatment. Finally, livers and tumors extracted from mice were prepared for pathologic examination and immunohistochemical (IHC) staining on day 21. Tumor weights of mice were also recorded. The flow chart of our experimental protocol is summarized in Figure 5.

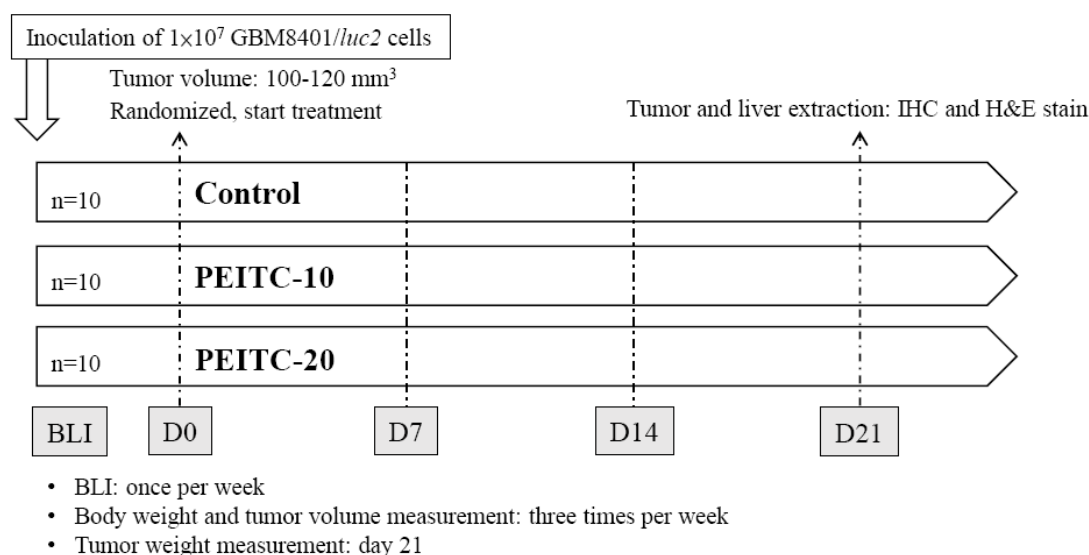


**Figure 5.** Experimental design for the treatments of human GBM 8401-bearing mice. Each mouse was injected with  $1 \times 10^7$  GBM 8401/*luc2* cells. After the tumor volume reached 100–120 mm<sup>3</sup>, mice were randomized into three different treatment groups (n = 10 per group). PEITC (10, 20  $\mu$ mole/100  $\mu$ L PBS) was administered daily by gavage. All mice were sacrificed 21 days after treatments. IHC: immunohistochemical.

#### 4.5. In Vivo Bioluminescent Imaging (BLI)

Mice tumor growth was also monitored by BLI once per week during treatment progress. Intraperitoneal injections of 150 mg/kg of D-luciferin (Promega, Madison, WI, USA) were administered to mice from each group 15 min before BLI scanning. During the scanning procedure, mice were anesthetized at 1–3% isoflurane dosage and emitted photons were recorded by a Xenogen IVIS imaging system 200 as described previously [32]. The acquisition period was 1 s, and then the signals emitted from the regions of interest were quantified by Living Image software (Version 2.20, Xenogen, Alameda, CA, USA) [34].

#### 4.6. IHC Staining and Pathological Examination

Mice were sacrificed on day 21, and tumors and livers were extracted. Tumors and livers were both fixed with 4% paraformaldehyde (PFA) at 4 °C for 24 h. Paraffin-embedded tumor tissues and liver tissue were sliced at 5 µm thickness by Bio-Check Laboratories Ltd. (New Taipei City, Taiwan). The IHC and hematoxylin and eosin (H&E) staining protocols were performed according to the manufacturer's recommendations. For immunohistochemical staining, primary antibodies including MCL-1, XIAP, Bax, and active Caspase-3 antibodies were added, respectively. An H&E staining kit from Bio-Check Laboratories Ltd. was used to stain slices. All slices were finally mounted with Prolong Gold Antifade reagent (ThermoFisher Scientific, Waltham, MA) and were imaged by microscopy-based TissueFAXS platform (TissueGnostics, Vienna, Austria) at 100× magnification [35]. Positive expression of MCL-1, XIAP, caspase-3, and Bax on IHC indices in tumor tissues was quantified with ImageJ software version 1.50 (National Institutes of Health, Bethesda, MD, USA) [36].

#### 4.7. Statistical Analysis

All data were represented with the mean ± standard error. One-way ANOVA with Newman–Keuls multi-comparison test was used for the comparison between PEITC-treated and control groups, and between PEITC-treated groups. Difference between the means was considered significant if  $p < 0.05$  or less.

**Author Contributions:** Conceptualization, J.-G.C.; Methodology, J.-G.C. and F.-T.H.; Software, Y.-C.C. and F.-T.H.; Validation, all authors; Formal Analysis, F.-T.H.; Investigation, X.X.; Resources, J.-G.C.; Data Curation, all authors.; Writing—Original Draft Preparation, Y.-C.C.; Writing—Review & Editing, J.-G.C. and F.-T.H.; Visualization, all authors; Supervision, J.-G.C. and F.-T.H.

**Funding:** This research was funded by Ministry of Science and Technology, Taipei, Taiwan [MOST106-2314-B-075A-005].

**Acknowledgments:** Experiments and data analysis were performed in part through the use of the Medical Research Core Facilities Center, Office of Research & Development at China Medical University, Taichung, Taiwan, R.O.C.

**Conflicts of Interest:** The authors declare no conflicts of interest.

## References

1. Nassiri, F.; Aldape, K.; Zadeh, G. The multiforme of glioblastoma. *Neuro-Oncology* **2018**, *20*, 437–438. [[CrossRef](#)] [[PubMed](#)]
2. Moon, Y.J.; Brazeau, D.A.; Morris, M.E. Dietary phenethyl isothiocyanate alters gene expression in human breast cancer cells. *Evid. Based Complement. Alternat. Med.* **2011**. [[CrossRef](#)] [[PubMed](#)]
3. Palliyaguru, D.L.; Yuan, J.M.; Kensler, T.W.; Fahey, J.W. Isothiocyanates: Translating the Power of Plants to People. *Mol. Nutr. Food Res.* **2018**. [[CrossRef](#)] [[PubMed](#)]
4. Gutierrez, S.E.; Romero-Oliva, F.A. Epigenetic changes: A common theme in acute myelogenous leukemogenesis. *J. Hematol. Oncol.* **2013**, *6*, 57. [[CrossRef](#)] [[PubMed](#)]
5. Cang, S.; Ma, Y.; Chiao, J.W.; Liu, D. Phenethyl isothiocyanate and paclitaxel synergistically enhanced apoptosis and alpha-tubulin hyperacetylation in breast cancer cells. *Exp. Hematol. Oncol.* **2014**, *3*, 5. [[CrossRef](#)] [[PubMed](#)]
6. Cang, S.; Xu, X.; Ma, Y.; Liu, D.; Chiao, J.W. Hypoacetylation, hypomethylation, and dephosphorylation of H2B histones and excessive histone deacetylase activity in DU-145 prostate cancer cells. *J. Hematol. Oncol.* **2016**, *9*, 3. [[CrossRef](#)] [[PubMed](#)]
7. Han, S.; Kim, Y.J.; Lee, J.; Jeon, S.; Hong, T.; Park, G.J.; Yoon, J.H.; Yahng, S.A.; Shin, S.H.; Lee, S.E.; et al. Model-based adaptive phase I trial design of post-transplant decitabine maintenance in myelodysplastic syndrome. *J. Hematol. Oncol.* **2015**, *8*, 118. [[CrossRef](#)] [[PubMed](#)]
8. Gupta, P.; Wright, S.E.; Kim, S.H.; Srivastava, S.K. Phenethyl isothiocyanate: A comprehensive review of anti-cancer mechanisms. *Biochim. Biophys. Acta* **2014**, *1846*, 405–424. [[CrossRef](#)] [[PubMed](#)]

9. Chou, Y.C.; Chang, M.Y.; Wang, M.J.; Harnod, T.; Hung, C.H.; Lee, H.T.; Shen, C.C.; Chung, J.G. PEITC induces apoptosis of Human Brain Glioblastoma GBM8401 Cells through the extrinsic- and intrinsic-signaling pathways. *Neurochem. Int.* **2015**, *81*, 32–40. [[CrossRef](#)] [[PubMed](#)]
10. Chou, Y.C.; Chang, M.Y.; Wang, M.J.; Yu, F.S.; Liu, H.C.; Harnod, T.; Hung, C.H.; Lee, H.T.; Chung, J.G. PEITC inhibits human brain glioblastoma GBM 8401 cell migration and invasion through the inhibition of uPA, Rho, A., and Ras with inhibition of MMP-2, -7 and -9 gene expression. *Oncol. Rep.* **2015**, *34*, 2489–2496. [[CrossRef](#)] [[PubMed](#)]
11. Chou, Y.C.; Chang, M.Y.; Wang, M.J.; Liu, H.C.; Chang, S.J.; Harnod, T.; Hung, C.H.; Lee, H.T.; Shen, C.C.; Chung, J.G. Phenethyl isothiocyanate alters the gene expression and the levels of protein associated with cell cycle regulation in human glioblastoma GBM 8401 cells. *Environ. Toxicol.* **2017**, *32*, 176–187. [[CrossRef](#)] [[PubMed](#)]
12. Ni, W.Y.; Lu, H.F.; Hsu, S.C.; Hsiao, Y.P.; Liu, K.C.; Liu, J.Y.; Ji, B.C.; Hsueh, S.C.; Hung, F.M.; Shang, H.S.; et al. Phenethyl isothiocyanate inhibits in vivo growth of subcutaneous xenograft tumors of human malignant melanoma A375.S2 cells. *In Vivo* **2014**, *28*, 891–894. [[PubMed](#)]
13. Fuentes, F.; Paredes-Gonzalez, X.; Kong, A.N. Dietary glucosinolates sulforaphane, phenethyl isothiocyanate, indole-3-carbinol/3,3'-diindolylmethane: Anti-oxidative stress/inflammation, Nrf2, epigenetics/epigenomics and in vivo cancer chemopreventive efficacy. *Curr. Pharmacol. Rep.* **2015**, *1*, 179–196. [[CrossRef](#)] [[PubMed](#)]
14. Ramalho-Carvalho, J.; Graca, I.; Gomez, A.; Oliveira, J.; Henrique, R.; Esteller, M.; Jeronimo, C. Downregulation of miR-130b~301b cluster is mediated by aberrant promoter methylation and impairs cellular senescence in prostate cancer. *J. Hematol. Oncol.* **2017**, *10*, 43. [[CrossRef](#)] [[PubMed](#)]
15. Izzotti, A.; Calin, G.A.; Steele, V.E.; Cartiglia, C.; Longobardi, M.; Croce, C.M.; De Flora, S. Chemoprevention of cigarette smoke-induced alterations of MicroRNA expression in rat lungs. *Cancer Prev. Res.* **2010**, *3*, 62–72. [[CrossRef](#)] [[PubMed](#)]
16. Cheung, K.L.; Khor, T.O.; Huang, M.T.; Kong, A.N. Differential in vivo mechanism of chemoprevention of tumor formation in azoxymethane/dextran sodium sulfate mice by PEITC and DBM. *Carcinogenesis* **2010**, *31*, 880–885. [[CrossRef](#)] [[PubMed](#)]
17. Levenson, J.D.; Zhang, H.; Chen, J.; Tahir, S.K.; Phillips, D.C.; Xue, J.; Nimmer, P.; Jin, S.; Smith, M.; Xiao, Y.; et al. Potent and selective small-molecule MCL-1 inhibitors demonstrate on-target cancer cell killing activity as single agents and in combination with ABT-263 (navitoclax). *Cell Death Dis.* **2015**. [[CrossRef](#)] [[PubMed](#)]
18. Szegezdi, E.; Macdonald, D.C.; Ni Chonghaile, T.; Gupta, S.; Samali, A. Bcl-2 family on guard at the ER. *Am. J. Physiol. Cell Physiol.* **2009**, *296*, 941–953. [[CrossRef](#)] [[PubMed](#)]
19. Zhang, Y.; Ishida, C.T.; Ishida, W.; Lo, S.L.; Zhao, J.; Shu, C.; Bianchetti, E.; Kleiner, G.; Sanchez-Quintero, M.; Quinzii, C.M.; et al. Combined HDAC and bromodomain protein inhibition reprograms tumor cell metabolism and elicits synthetic lethality in glioblastoma. *Clin. Cancer Res.* **2018**, *24*, 3941–3954. [[CrossRef](#)] [[PubMed](#)]
20. Song, Y.; Wu, F.; Wu, J. Targeting histone methylation for cancer therapy: Enzymes, inhibitors, biological activity and perspectives. *J. Hematol. Oncol.* **2016**, *9*, 49. [[CrossRef](#)] [[PubMed](#)]
21. Karpel-Massler, G.; Ishida, C.T.; Bianchetti, E.; Shu, C.; Perez-Lorenzo, R.; Horst, B.; Banu, M.; Roth, K.A.; Bruce, J.N.; Canoll, P.; et al. Inhibition of mitochondrial matrix chaperones and antiapoptotic Bcl-2 family proteins empower antitumor therapeutic responses. *Cancer Res.* **2017**, *77*, 3513–3526. [[CrossRef](#)] [[PubMed](#)]
22. Ghobrial, I.M.; Witzig, T.E.; Adjei, A.A. Targeting apoptosis pathways in cancer therapy. *CA A Cancer J. Clin.* **2005**, *55*, 178–194. [[CrossRef](#)]
23. Fulda, S.; Vucic, D. Targeting IAP proteins for therapeutic intervention in cancer. *Nat. Rev. Drug Discov.* **2012**, *11*, 109–124. [[CrossRef](#)] [[PubMed](#)]
24. Zappavigna, S.; Scutto, M.; Cossu, A.M.; Ingrosso, D.; De Rosa, M.; Schiraldi, C.; Filosa, R.; Caraglia, M. The 1,4 benzoquinone-featured 5-lipoxygenase inhibitor RF-Id induces apoptotic death through downregulation of IAPs in human glioblastoma cells. *J. Exp. Clin. Cancer Res.* **2016**, *35*, 167. [[CrossRef](#)] [[PubMed](#)]
25. Tchoghndjian, A.; Souberan, A.; Tabouret, E.; Colin, C.; Denicolai, E.; Jiguet-Jiglaire, C.; El-Battari, A.; Villard, C.; Baeza-Kallee, N.; Figarella-Branger, D. Inhibitor of apoptosis protein expression in glioblastomas and their in vitro and in vivo targeting by SMAC mimetic GDC-0152. *Cell Death Dis.* **2016**, *7*. [[CrossRef](#)] [[PubMed](#)]

26. Jin, Z.; El-Deiry, W.S. Overview of cell death signaling pathways. *Cancer Biol. Ther.* **2005**, *4*, 139–163. [[CrossRef](#)] [[PubMed](#)]
27. McIlwain, D.R.; Berger, T.; Mak, T.W. Caspase functions in cell death and disease. *Cold Spring Harb. Perspect. Biol.* **2013**, *5*. [[CrossRef](#)] [[PubMed](#)]
28. Zhong, D.; Zhao, S.; He, G.; Li, J.; Lang, Y.; Ye, W.; Li, Y.; Jiang, C.; Li, X. Stable knockdown of LRG1 by RNA interference inhibits growth and promotes apoptosis of glioblastoma cells in vitro and in vivo. *Tumour Biol.* **2015**, *36*, 4271–4278. [[CrossRef](#)] [[PubMed](#)]
29. Seo, K.W.; Kim, J.G.; Park, M.; Kim, T.W.; Kim, H.J. Effects of phenethylisothiocyanate on the expression of glutathione S-transferases and hepatotoxicity induced by acetaminophen. *Xenobiotica* **2000**, *30*, 535–545. [[CrossRef](#)] [[PubMed](#)]
30. Wang, D.Y.; Yeh, C.C.; Lee, J.H.; Hung, C.F.; Chung, J.G. Berberine inhibited arylamine N-acetyltransferase activity and gene expression and DNA adduct formation in human malignant astrocytoma (G9T/VGH) and brain glioblastoma multiforms (GBM 8401) cells. *Neurochem. Res.* **2002**, *27*, 883–889. [[CrossRef](#)] [[PubMed](#)]
31. Tsai, J.J.; Pan, P.J.; Hsu, F.T. Regorafenib induces extrinsic and intrinsic apoptosis through inhibition of ERK/NF-kappaB activation in hepatocellular carcinoma cells. *Oncol. Rep.* **2017**, *37*, 1036–1044. [[CrossRef](#)] [[PubMed](#)]
32. Hsu, F.T.; Liu, Y.C.; Chiang, I.T.; Liu, R.S.; Wang, H.E.; Lin, W.J.; Hwang, J.J. Sorafenib increases efficacy of vorinostat against human hepatocellular carcinoma through transduction inhibition of vorinostat-induced ERK/NF-kappaB signaling. *Int. J. Oncol.* **2014**, *45*, 177–188. [[CrossRef](#)] [[PubMed](#)]
33. Della Peruta, M.; Badar, A.; Rosales, C.; Chokshi, S.; Kia, A.; Nathwani, D.; Galante, E.; Yan, R.; Arstad, E.; Davidoff, A.M.; et al. Preferential targeting of disseminated liver tumors using a recombinant adeno-associated viral vector. *Hum. Gene Ther.* **2015**, *26*, 94–103. [[CrossRef](#)] [[PubMed](#)]
34. Workman, P.; Aboagye, E.O.; Balkwill, F.; Balmain, A.; Bruder, G.; Chaplin, D.J.; Double, J.A.; Everitt, J.; Farningham, D.A.; Glennie, M.J.; et al. Guidelines for the welfare and use of animals in cancer research. *Br. J. Cancer* **2010**, *102*, 1555–1577. [[CrossRef](#)] [[PubMed](#)]
35. Hsu, F.T.; Chang, B.; Chen, J.C.; Chiang, I.T.; Liu, Y.C.; Kwang, W.K.; Hwang, J.J. Synergistic effect of sorafenib and radiation on human oral carcinoma in vivo. *Sci. Rep.* **2015**, *5*, 15391. [[CrossRef](#)] [[PubMed](#)]
36. Tsai, J.J.; Hsu, F.T.; Pan, P.J.; Chen, C.W.; Kuo, Y.C. Amentoflavone enhances the therapeutic efficacy of sorafenib by inhibiting anti-apoptotic potential and potentiating apoptosis in hepatocellular carcinoma in vivo. *Anticancer Res.* **2018**, *38*, 2119–2125. [[PubMed](#)]

**Sample Availability:** Samples of the compounds phenethyl isothiocyanate (PEITC) are available from the authors.



© 2018 by the authors. Licensee MDPI, Basel, Switzerland. This article is an open access article distributed under the terms and conditions of the Creative Commons Attribution (CC BY) license (<http://creativecommons.org/licenses/by/4.0/>).